ALT 12
Advanced Laser Technologies
2 – 6 September 2012, Thun, Switzerland

ALT 12
c/o Bern University of Applied Sciences
Engineering and Information Technology
Pestalozzistrasse 20, CH-3400 Burgdorf
info@alt12.org, www.alt12.org
0041 (0) 34 426 42 06

INFRARED BROADBAND SOURCE FROM 1000NM TO 1700NM, BASED ON AN ERBIUM, NEODYMIUM AND BISMUTH DOPED DOUBLE-CLAD FIBER

Authors:

S. Pilz, D. Etissa, C. Barbosa, V. Romano

DOI: 10.12684/alt.1.73

Corresponding author: S. Pilz

e-mail: soenke.pilz@bfh.ch

Infrared broadband source from 1000nm to 1700nm, based on an Erbium, Neodymium and Bismuth doped double-clad fiber

S. Pilz[1], D. Etissa[1], C. Barbosa[2] and V.Romano[3]

[1]Institute of Applied Physics, University of Bern, Sidlerstrasse 5,
CH-3012 Bern, Switzerland
[2]Instituto de Estudos Avancados (IEAv), Sao Jose dos Campos, Rod. Dos Tamoios,
SP Sao Paulo, Brazil
[3]Bern University of Applied Sciences, ALPS, Pestalozzistrasse 20,
CH-3400 Burgdorf, Switzerland

Abstract

A Nd^{3+}, Er^{3+} and Bi^{3+} doped double-clad fiber (core diameter of 25.5μm, cladding diameter of 125μm) with a broad infrared emission has been fabricated based on technique of dry granulated oxides and investigated. Upon the excitation with a 800nm cw pump source all of the three dopant materials showed fluorescence in the infrared region of interest (1000-1700nm). The observed emitted fluorescence power was measured to be 659μW. Changing the pump wavelength to 976nm led to a fluorescence of only Er^{3+} and Bi^{3+} and a broadening of the Bi^{3+} emission peak. The maximal measured fluorescence output power was 1.42mW, when pumped at 976nm.

Introduction

Broadband light sources have become indispensable for a multitude of applications, among them spectroscopy, microscopy, sensing or medical diagnosis [1,2,3]. Many of the applications rely on the very short coherence length which is a consequence of the broad spectral distribution and which may be as short as a few microns.

Usually employed broadband light sources are thermal light sources, light emitting diodes, super luminescence diodes, amplified spontaneous emission and super-fluorescent fiber sources, femtosecond oscillators or white light sources based on nonlinear continuum generation. Other sources, such as very long Raman fiber lasers, have been investigated but are not as widespread. While most light sources have bandwidths of less than 100nm, some are as broad as a couple of hundred nm. Because of their superior beam quality and high spatial coherence fiber based sources, most prominently super-fluorescent rare earth doped or highly nonlinear fibers, are often preferred to other sources. A further important characteristic is the output power of a light source. Generally, the broadest bandwidth but also the lowest output power is reached with spontaneous emission. Amplified spontaneous emission has a higher power but shows some narrowing of the spectra depending on the degree of amplification. Finally, the highest output power is reached with laser emission, but in continuous wave (cw) operation this comes at the cost of a considerably reduced bandwidth. Nevertheless, even in the case of cw laser activity, laser emission can cover a range of 50nm in the case of a Nd^{3+}:Al^{3+}:glass fibers or 75nm for a Yb^{3+}:Al^{3+}:glass fiber. The broadest bandwidths and the highest output powers, however, are undoubtedly reached with standalone mode-locked oscillators or with subsequent continuum generation, but at the expense of high costs.

In a previous paper [4], we reported on an extremely broadband continuous wave fluorescence light source, which is based on a fiber with a single, multiply doped core pumped by a single pump wavelength.

Here, we report on another fiber realized by the same production method, the powder in tube method, and where we targeted the region above 1000nm for emission. The envisaged use of the fiber is in the field of broadband amplification. To that end the rare earths Erbium and Neodymium as well as the transition element Bismuth were chosen as active dopants. Aluminum was added to enhance the solubility of the rare earths.

Fabrication Procedure And Geometry

The fabrication of the fiber is based upon the technique of dry granulated oxides [5] and was produced at the IAP (Institute of Applied Physics, University of Bern). The doped core-area of the fiber is composed of a mixture of granulated silica (SiO_2), rare earth oxides (Er_2O_3, Nd_2O_3) and metal oxides (Bi_2O_3, Al_2O_3). Bismuth-, Erbium- and Neodymium-oxide were chosen to optimize the generation of fluorescence in the spectral range between 1000 and 1700nm [5,6,7,8,9,10,11,12].

The composition of the core-mixture consisted of 98.57*at.%* of SiO_2, 1.3*at.%* of Al_2O_3, 0.1*at.%* of Bi_2O_3, 0.02*at.%* Er_2O_3 and 0.01*at.%* Nd_2O_3 (see Table 1). Aluminum is used to increase the refractive index of the core compared to the cladding and to improve the solubility of the dopant material [8]. Another benefit of Aluminum is that it prevents the rare earth ions from clustering. Co-doping with 1.3*at.%* leads to a refractive index step (Δn) smaller than 0.0046 and to a numerical aperture NA_{core} smaller than 0.115 (see Subsection *Refractive Index Of The Core*). This core-mixture powder was melted and vitrified with the aid of a CO_2-Laser. After the vitrification the mixture was roughly milled. The procedure of melting, vitrifying and milling was repeated three times all in all to increase the homogeneity. The resulting vitrified material mixture was filled into a silica tube with an inner diameter of 17*mm* and an outer diameter of 21*mm*. This preform was drawn to a fiber-rod with a diameter of approximately 2.4*mm*. This fiber-rob was placed and centered in a second 17*mm* by 21*mm* silica tube and became the fiber-core of the active fiber.

The remaining space of the second preform was filled up with undoped granulated silica (n_{SiO_2}=1.45). Together with the walls of the first and second silica tube, the undoped granulated silica became the cladding. This preform was drawn to a fiber with 125μm cladding diameter and ≈25.5μm core diameter. The diameters were determined on the one hand by coupling a white light source into the fiber and contemplating the opposite fiber end with a microscope (see Figure 1 b)). Since the doped core absorbs a part of the white light source, there is a brightness difference between the core and cladding area and one can determine the core and the cladding diameters (Figure 1 b)). On the other hand a fiber-coupled 800*nm* pump-diode was spliced to the fiber and the fiber end was imaged to a CCD camera (Pulnix: TM9701). Figure 1 c) shows the pump light distribution at the fiber end. As one can see, the pump light is absorbed in the core region. By using two long pass 1000*nm* filters (Thorlabs FEL1000) the pump light is blocked and only the infrared fluorescence generated in the core and guided by the fiber is imagined to the CCD (see Figure 1 d)). Since the used CCD camera is based on a silicon chip with a spectral response until 1100*nm*, Figure 1 d) only shows the fluorescence in the range between 1000 and 1100*nm*.

The fiber was coated with a low refractive index acrylate (SSCP Corp., PC-373, n_{coat}=1.389) to achieve also a waveguide structure for the cladding, which results in a so called double-clad fiber (DCF). The total fiber diameter including the coating was ≈400μm. The numerical aperture of the cladding is given by the refractive index of the coating and cladding by

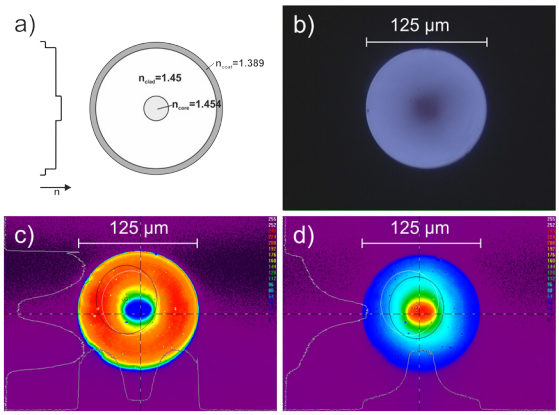

Figure 1: a) Geometry and refractive indices of the active double-clad fiber structure; b) microscope image of the fiber end by injecting a white light source; c) 800*nm* pump light and d) fluorescence distribution of the fiber by imaging the fiber end onto a CCD.

$$NA_{clad} = \sqrt{n_{clad}^2 - n_{coat}^2} = 0.41. \qquad (1)$$

Due to the double-clad structure the pump light can be coupled into the cladding (cladding pumping) and enables the use of multimode pump sources, such as high power pump diodes with a low brightness. The fluorescence of the doped material generated in the core is uniformly emitted into 360° which is equivalent to a solid angle of Ω=4π *rad*. The solid angle is defined by

$$\Omega = \frac{S}{r^2} = 2\pi[1-\cos(\alpha)] = 4\pi \sin^2\left(\frac{\alpha}{2}\right), \qquad (2)$$

where *S* is a part of the surface of a sphere and *r* the radius (see Figure 2). Furthermore, α is the divergence half-angle given by

$$NA = \sin(\alpha) \qquad (3)$$

with the assumption that the numerical aperture is measured in an air environment (n_{air}=1). The fraction ε_{core} of the generated fluorescence photons that are guided in the core and propagate towards one fiber end is given by

$$\varepsilon_{core} < \frac{\Omega_{core}}{4\pi} = \sin^2\left(\frac{\sin^{-1}(NA_{core})}{2}\right) \approx 0.335\%. \qquad (4)$$

Since the fiber is a waveguide with two propagation directions, the same amount of fluorescence light propagates in the opposite direction in the core. The remaining fluorescence light escapes the core and a part of it is guided in the cladding. The fraction ε_{clad} guided by the cladding towards one fiber end is

$$\varepsilon_{clad} < \sin^2\left(\frac{\sin^{-1}(NA_{clad})}{2}\right) - \sin^2\left(\frac{\sin^{-1}(NA_{core})}{2}\right) \approx 4.2\%. \qquad (5)$$

In the used setup configuration, we can only measure the light that is propagation in one direction. An amount of about 90.93% of the generated fluorescence laterally leaks from the fiber, because it cannot be guided by the waveguide structure of the fiber.

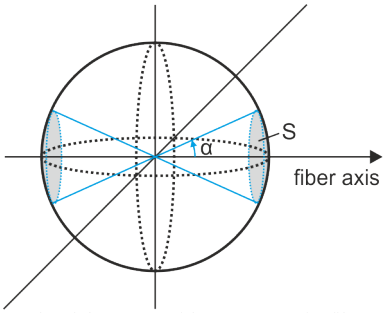

Figure 2: Solid angle of the waveguide structure of a fiber with a divergence half-angle α. The generated florescence photons can propagate through the fiber in two directions, if its direction of propagation α lies inside the solid angle defined by the NA of the fiber.

Measurements

Refractive Index Of The Core

With the aid of the XLIM (University of Limoges) a transversal refractive index scan of an uncoated fiber piece (fiber B) with a similar doping was done. The difference in doping concentrations can be seen in Table 1 and the result of the refractive index measurement is shown in Figure 3. The refractive index difference between the core and the cladding is $\Delta n_B \approx 0.0046$ for fiber B, leading to a numerical aperture of

$$NA_{core,B} = \sqrt{n_{core}^2 - n_{clad}^2} = \sqrt{2n_{core}\Delta n + \Delta n^2} = 0.1156. \quad (6)$$

The decrease of the doping concentration for fiber A lowers the refractive index difference ($\Delta n = \Delta n_A < 0.0046$) and the numerical aperture, thus we can write

$$NA_{core} = NA_{core,A} < 0.1156. \quad (7)$$

Table 1: Doping concentration of fiber A and B.

	Fiber A [at.%]	Fiber B [at.%]
AL_2O_3	1.3	3.0
Bi_2O_3	0.1	0.4
Er_2O_3	0.02	0.04
Nd_2O_3	0.01	0.05
SiO_2	98.57	96.51

As a result of the large fiber core the fiber A does not fulfill the single-mode condition anymore, which is given by

$$V = \frac{2\pi r_{core} NA_{core}}{\lambda} \leq 2.4048, \quad (8)$$

where V is the normalized frequency, which is often referred as V-number. Thus, the guidance of the core is not single-mode, it is multimode. In the upcoming experiments we used fiber A for all measurements.

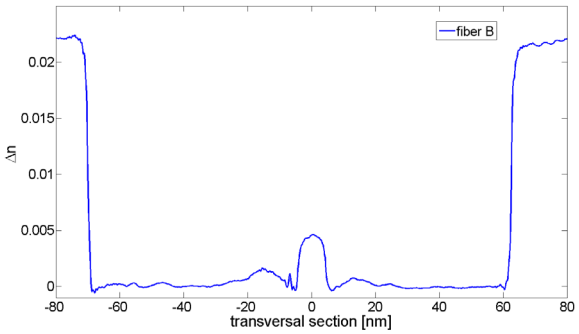

Figure 3: Refractive index measurement of fiber B, the difference between core and cladding is ~0.0046.

Experimental Setup And Pump Configuration

The dopant material was chosen, because the chosen rare earths (Er, Nd) and transition element (Bi) can be simultaneously excited with a pump wavelength around 800*nm* [7,8,10,12]. The self-made active fiber was spliced to a 4/125*µm* DC output-fiber (NA = 0.45) of a fiber-combiner (see Figure 4. The combiner (Gooch&Housego: TFB-064212A71) is a 2+1x1 combiner, which has two standard pump-input-fibers with 105/125*µm* (with NA 0.22) and a signal input fiber with a 4*µm* core. The output-fiber is a 4/125*µm* double clad fiber with a numerical aperture of the cladding of 0.45. In this setup only the pump-input-fibers and the output-fiber is used.

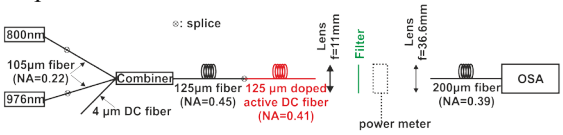

Figure 4: Power and spectral measurement setup.

Fiber Characterization

For characterization of the active DC fiber we spliced two commercially available, fiber-coupled (105/125*µm*, NA=0.15) laser modules to the pump-input-fibers of the combiner. One pump module is emitting around 800*nm* (Oclaro: MU8-808-01) and the other at 976*nm* (Oclaro: MU6-975-04). Since we go from a smaller diameter and NA to a bigger diameter and NA (at the splice between pump modules and combiner) we were able to produce a low-loss splice between them. At the splice between the combiner and the active fiber the diameter matches, but the NA of the combiner-output is bigger than the NA of the active fiber, therefore we lose a fraction of the pump power at this splice. For the determination of the splice-loss, we have measured the pump power coming directly out of the combiner-output-fiber and the cw pump power coming directly out of a 6.3*cm* long active

fiber piece spliced to the combiner-output-fiber. The 6.3*cm* long active fiber piece is the shortest piece of a cutback measurement. The theoretical transmission T_t of a splice from a higher low to a NA is $T_t=(NA_{low}/NA_{high})^2=(0.41/0.45)^2\approx 83.01\%$. We assume that in such a short double-clad active fiber piece, the absorption of the pump as a result of the dopant material is negligible compared with the residual pump light and that the difference in the power output only arises due to the NA mismatch and the splice itself. For that reason we assume that the measured residual pump power coming out of the 6.3*cm* long active fiber piece is equal to the inserted pump power in consideration of the splice and NA losses, and therefore this value is the pump power inserted in the active fiber (see Table 2).

The two pump modules were controlled in temperature by a TEC-controller (arroyo instruments: 5310). The 800*nm* diode was always operated at 20°*C* for different pump-currents. Due to the increasing pump-current with constant TEC, the peak-wavelength of the emission shifts to higher wavelengths, as can be seen in Figure 5. Since this shift is not large, and the absorption of the dopant materials around 800*nm* is quite broad [8,10], we did not have to stabilize the emission peak wavelength at 800*nm*. For the 976*nm* diode we fixed the emission wavelength peak at 976*nm* by changing the temperature of the TEC for increasing currents, as can be seen in Table 2.

Table 2: Pump power as a function of pump current, temperature of the TEC and wavelength.

Diode	I[*A*]	T_{TEC} [°*C*]	P_{pump} [*mW*]
MU8-808-01	1	20	291
MU8-808-01	3	20	2210
MU8-808-01	5	20	3760
MU6-975-04	1	30	431
MU6-975-04	2	22	1972
MU6-975-04	5	15	3430

The residual pump light and the fluorescence, which are guided by the core and cladding, are collimated with a lens (f=11*mm*). The power of the collimated beam is measured with a thermal power meter (Ophir: 3A-FS and/or 10A-V1) and filtered with three long pass filters (Thorlabs: FEL1000, 80% averaged transmittance above 1000*nm*) for infrared (IR) fluorescence measurements. The measured and averaged transmittance of the collimating optic T_c is ca. 91.25%. Since the fluorescence power is negligible small (at least an order of 10^{-4} smaller) compared to the residual pump light, the residual pump power is measured without any filter. For spectral measurements of the IR fluorescence, the collimated and filtered beam is focused with a lens (f=36.6*mm*) onto a multimode-fiber with a core diameter of 200μm and a NA of 0.39. The multimode-fiber guides the light to an optical spectrum analyzer OSA (Yokogawa: AQ6370, resolution 0.5nm).

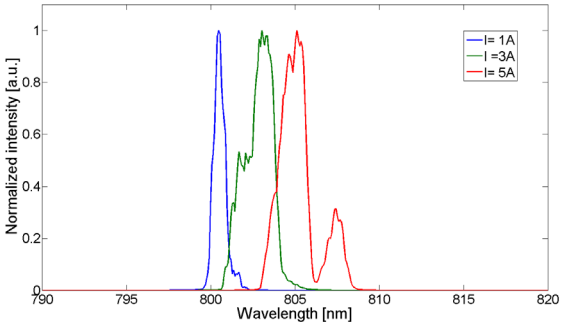

Figure 5: Red shift of the emission of the 800*nm* diode due to the increase of the pump-current at constant temp (20°*C*).

All power measurements were corrected with the averaged transmittance of the collimating optic $T_c=0.9125$ and supplementary the infrared fluorescence power was corrected by the averaged transmittance of the three long pass filters $T_F = 0.8^3=0.512$. Thus the powers are given by

$$P_{out,residualpump} = T_c^{-1} P_{meas,residualpump} \qquad (10)$$

$$P_{out,IR} = T_c^{-1} T_F^{-1} P_{meas,IR}\,. \qquad (11)$$

For the investigation of the spectral characteristics and the power output of the active fiber, we did a cutback measurement. We measured the spectrum and the power of the infrared fluorescence generated from the dopant material and guided by the fiber (core and cladding) as well as the residual pump power for four different fiber lengths, at two pump wavelengths each with three various pump currents.

First we excited a 9.96*m* long active fiber piece with 3.76*W* at 800*nm* using the setup presented in Figure 4. Figure 6 shows the measured spectral shape from 1000 till 1700*nm*. In order to protect the OSA from residual pump light we used three long pass 1000*nm* Filter (FEL1000). The fluorescence light in the visible range (below 1000*nm*) generated by excited state absorption (ESA) and/or energy transfer up-conversion (ETU) was blocked too by the filters. The four main peaks in the spectrum can be identified. The peak at 1060*nm* can be chalked up to the transition $^4F_{3/2} \rightarrow {}^4I_{11/2}$ of the Nd^{3+} [6]. The Nd^{3+} is also responsible for the peak at 1333*nm*, the associated transition is $^4F_{3/2} \rightarrow {}^4I_{13/2}$ [6]. Er^{3+} produces the peak at 1531*nm*, corresponding to the $^4I_{13/2} \rightarrow {}^4I_{15/2}$ transition [6]. Bi^{3+} is responsible for the peak around 1100*nm* [10,11,12]. Taking the T_c and T_F into account the emitted power $P_{out,IR}$ (guided and emitted from the cladding and the core) in the spectral range above 1000*nm* (see Figure 6) is 659.25μW, when pumped with 3.76*W*. The corresponding fluorescence, which is only guided and emitted by the core is $P_{out,IR,core}=P_{out,IR}*\varepsilon_{core}/(\varepsilon_{core}+\varepsilon_{clad})=48.7\mu W$. The corresponding residual pump power $P_{out,residual\ pump}$ emitted by the fiber is 2.09*W*.

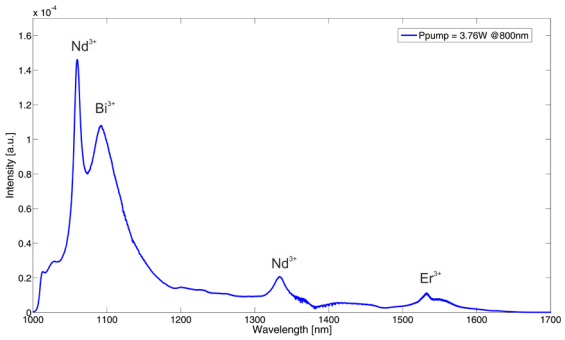

Figure 6: Fluorescence spectrum of a 9.96*m* long fiber piece pumped at 800*nm* with 3.76*W*. The peaks are labeled with the corresponding dopant material.

Figure 7 shows the evolution of the spectral shape for the cutback measurement. We investigated the fiber output at four lengths (9.96, 7.0, 4.0 and 0.99*m*) and for three different pump powers at 800*nm*. It has to be mentioned that the coupling into the 200μm fiber of the OSA was not constant due to varying cleaves for different fiber lengths. Therefore the intensity amplitudes of the spectra for different fiber lengths are not comparable.

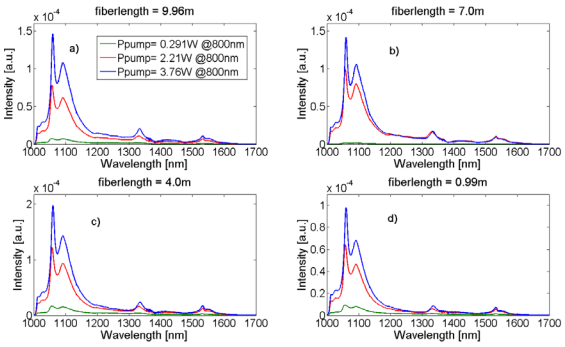

Figure 7: Spectra of a) a fiber length of 9.96*m*, b) a fiber length of 7.0*m*, c) a fiber length of 4.0*m* and d) a fiber length of 0.99*m* for three different pump powers at 800*nm*.

Changing the pump wavelength from 800 to 976*nm* has consequences for the spectrum. Nd^{3+} has no absorption at all at 976*nm*. The absorption (respectively the absorption cross section) of Er^{3+} is stronger at 976 than at 800*nm* [8]. Bi^{3+} also absorbs at 976*nm* [10,12]. If we compare the both spectra generated by 800 and 976*nm* pump diodes, we observe that the emission from Er^{3+} is stronger for pumping at 976*nm* (see Figure 8). This is in a good agreement with the fact of a smaller absorption cross section for 800*nm* excitation, even if the pump power at a constant pump current of 5*A* for 976*nm* ($P_{pump,976}$=3.43*W*) is smaller as for 800*nm* ($P_{pump,800}$=3.76*W*). The both Nd^{3+} peaks vanish for 976*nm* pumping, due to the fact of no absorption at 976*nm*. The Bi^{3+} peak is broader for 976*nm* excitation compared with 800*nm*. The photoluminescence (PL) power guided and emitted from the core and cladding $P_{out,IR}$ was 1423.37μW, when pumped with 3.43*W* at 976*nm*. This corresponds to a power of $P_{out,IR,core}=P_{out,IR}*\varepsilon_{core}/(\varepsilon_{core}+\varepsilon_{clad})$=105.1$\mu W$, which is guided and emitted only from the core. The corresponding residual pump power at this fiber length was $P_{out,residual\ pump}$=1.77*W*.

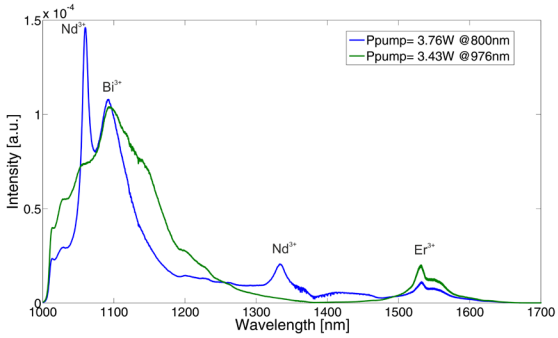

Figure 8: Comparison between the IR-fluorescence spectra of a 9.96*m* long fiber piece for a 800*nm* ($P_{pump,800}$=3.76W) and a 976*nm* ($P_{pump,976}$=3.43*W*) pump wavelength.

During the cutback measurements we did not only use the 800*nm* pump diode, we also used the 976*nm* diode. The spectra for excitation at 976*nm* are shown in Figure 9. As already mentioned for 800*nm* excitation the coupling into the 200μm fiber is not at all constant, and therefore the intensity amplitudes are also not comparable for the various fiber lengths for 976*nm* pumping. The plot in Figure 10 summarizes the observed overall fluorescence power emitted and guided by the fiber doing the cutback for different pump powers and pump wavelengths. In addition to the pump wavelength dependence of the fluorescence spectrum, the spectral power density could also be shifted from the infrared to the visible as function of the fiber length or the pump power due to the ESA and/or ETU. Thus and since we have only observed the infrared fraction of the fluorescence, we are not able to make a good conclusion about the measured spectral shape and the corresponding power.

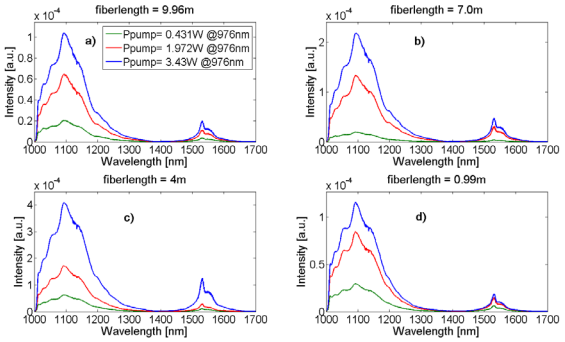

Figure 9: Spectra of a) a fiber length of 9.96*m*, b) a fiber length of 7.0*m*, c) a fiber length of 4.0*m* and d) a fiber length of 0.99*m* for three different pump powers at 976*nm*.

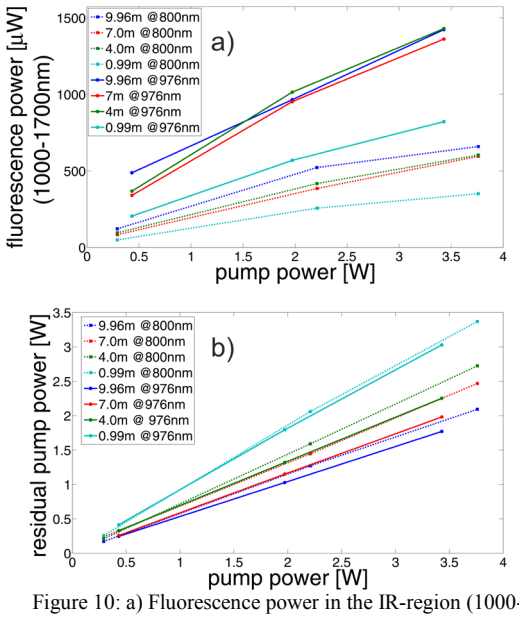

Figure 10: a) Fluorescence power in the IR-region (1000-1700*nm*) for 800 and 976*nm* excitation and for different pump powers, b) the corresponding residual pump power.

Conclusion

To conclude, with the goal of a broadband fluorescence in the infrared region from 1000 to 1700*nm* we manufactured an active doped double-clad fiber based upon the technique of dry granulated oxides, with a broad emission in the region of 1000 to 1700*nm*. We used the rare earth oxides Nd^{3+} and Er^{3+} as well as the metal oxides Bi^{3+} and Al^{3+} as dopant material for the core. The core diameter was 25.5μm and had a refractive index step of $\Delta n < 0.0046$, leading to a numerical aperture NA smaller than 0.1156. The cladding of the double clad structure had a diameter of 125µm and a NA of 0.41. Excitation with a 800*nm* fiber-coupled diode led to fluorescence of Nd^{3+}, Er^{3+} and Bi^{3+}. We measured an emitted power in the spectral range from 1000 till 1700*nm* of nearly 660μW for a fiber length of 9.96*m*, when pumped with 3.76*W* at 800*nm*. We demonstrated that only Er^{3+} and Bi^{3+} are excited when pumped with a 976*nm* pump source. We observed an emitted power of 1.42*mW* during pumping the same fiber piece with 3.43*W* of 976*nm* pump light.

Acknowledgments

The authors thank T. Schmidt and M. Neff for their help, arrangements and collaboration during the fabrication of the active double-clad fiber. J.L. Auguste we are grateful for the refractive index measurement. This project was made possible by the financial support of LIMAT and grants by the Centro Nacional de Pesquisa and the Instituto dos Estudos Avancados.

References

[1] Jacquemet, M., Picqué, N. et al., Continuous-wave 1.55µm diode-pumped surface emitting semiconductor laser for broadband multiplex spectroscopy, Optics Letters 32(11), 1387 (2007)

[2] Corle, T. R. and Kino, G. S., Confocal Scanning Optical Microscopy and Related Imaging Systems, Academic Press (1996)

[3] Martin-Lopez, S., Gonzalez-Herraez, M., Carrasco-Sanz, A. et al., Broadband spectrally flat and high power density light source for fibre sensing purposes, Measurement Science and Technology 17(5), 1014–1019 (2006)

[4] Di Labio, L., Lüthy, W., Romano, V., Sandoz, F., and Feurer, T., Superbroadband fluorescence fiber fabricated with granulated oxides, Optics Letters 33(10), 1050 (2008)

[5] Renner-Erny, R., Di Labio, L., and Lüthy, W., A novel technique for active fibre production, Optical Materials 29(8), 919–922 (2007)

[6] Di Labio, L., Lüthy, W., Romano, V., Feurer, T., and Sandoz, F., Broadband emitter based on a multiply RE-doped fiber, IAP Research Report No. 2008-0 (2008)

[7] Kaminskii, A. A., Laser Crystals: Their Physics and Properties , Springer, 1st ed. (1981)

[8] Digonnet, M. J., Rare-earth-doped fiber lasers and amplifiers , CRC Press, 2nd ed. (2001)

[9] Peng, M., Qiu, J., Chen, D., Meng, X., and Zhu, C., Superbroadband 1310nm emission from bismuth and tantalum codoped germanium oxide glasses," Optics Letters 30(18), 2433 (2005)

[10] Suzuki, T. and Ohishi, Y., Ultrabroadband near-infrared emission from Bi-doped Li_2O-Al_2O_3-SiO_2 glass, Applied Physics Letters 88(19), 191912 (2006)

[11] Neff, M., Metal and transition metal doped fibers, PhD thesis, University of Bern (2010)

[12] Dianov, E.M., Dvoyrin, V. V. et al., CW bismuth fibre laser, Quantum Electronics 35, 1083–1084 (Dec. 2005)